# Applicability of Drag Equation on a Dimpled Golf Ball using Changing Wind Velocities

Yutao Tang

The York school, Toronto, Canada

schangg47853@student.napavalley.edu

**Abstract.** The drag equation is commonly used to relate the resistance force experienced by an object traveling through fluids with its velocity. The pattern might vary based on the specific geometry of the objects (e.g., a dimpled golf ball). The dimples are known to reduce the amount of drag during the ball's flight through a series of complex aerodynamic processes. To investigate the ball's drag pattern, pressure and air velocity on the golf ball, a CFD using Ansys fluent is performed to simulate its aerodynamic features under nine different wind velocities. After the experiment, it was found that the relationship between the drag and velocity of the dimpled golf ball still generally conforms to the drag equation. The pressure and velocity distributions are consistent with the hypothesis, while the aerodynamic details are presented. The effect of dimples is also visualized, contributing to the flow demonstration. The investigation is valuable because the aerodynamic process of the dimpled sphere structure in changing wind velocities is well presented and analyzed, and it inspires further explorations on the aerodynamic effects of the dimple geometry.

**Keywords:** Golf ball, dimples, CFD, drag equation.

## 1. Introduction

Golf is strongly related to mechanics and dynamics (the body's movement), the interaction between the club and the ball, the material design and geometry for equipment, all of which require a scientific approach to optimize the game. After impacting, the ball flight trajectory concerns players as it displays their swing quality and outcome. During the flight, aerodynamics and fluid mechanics influence the ball's trajectory, determining its distance, height, spin and direction, which are all crucial components of a golf shot. An important factor that players consider when playing golf is the distance the ball flies, which is affected by the aerodynamic drag after launching [1]. In this paper, the specifics of golf ball geometry and air characteristics will be investigated to analyze their influences on the drag exerted on the golf ball and if the drag pattern conforms to the well-known drag equation and other occurring aerodynamic details. The dimples help reduce the drag force exerted on the golf ball, reducing the resistance the ball experiences during its flight [2, 3].

Plenty of studies have investigated the specifics of golf ball geometry traveling in airflow. A study in 2006 solidified the understanding of how dimples reduce drag by measuring the streamwise velocity above the dimpled surface [4]. The presence of dimples leads to increased turbulence intensity due to flow separation and instability of the shear layer when the ball travels through the air. As turbulence increases, the airflow attaches to the surface, wrapping around its back and overcoming strong resisting pressure gradients formed at the tail of the ball. This decreased pressure gradient results in less drag force. A study conducted in 2011 compared dimple size and diameter among balls from eight different manufacturers using a wind tunnel simulation lab [5]. The results revealed significant variations between samples, suggesting that dimpled structure can significantly affect ball flight. Further detailing the investigation, a research paper in 2016 investigates specifically the viscous drag experienced by the golf ball [6]. It discovers a positive correlation between surface roughness, a parameter defined as the ratio of dimple depth and ball diameter, and drag coefficient, an indicator of drag force, as a transition to lower Reynolds numbers was observed in the transcritical state when the surface roughness increases. Various methodologies are also used to study golf balls. A research in 2018 investigates the drag coefficient of the golf ball using a water tank and analyzed in Tracker [7]. Moreover, another investigation in 2007 looked into the relationship between dimple

figuration and noise levels using Fluent analysis software [8]. It is found that deeper dimples produce lower noise levels. This research inspires to simulate the golf ball specifics using Ansys fluent software. These studies show the exciting connection between aerodynamics and the sport, demonstrating room for further theoretical or modeling development.

This research will focus on the drag pattern of the dimpled golf ball and investigate its pressure and velocity configuration under changing wind velocities. Few online papers examine if a dimpled golf ball still conforms to the drag equation, as the dimples are commonly known to reduce drag significantly. They also did not present an accurate aerodynamic demonstration to show the details of the golf ball under varying wind velocities. In this paper, a CFD model will be established using Ansys fluent to qualitatively and quantitatively analyze the drag force experienced by the ball with changing wind velocities and to display the aerodynamic details. The paper will be divided into theoretical analysis, modeling set-up, experimental results and analysis, evaluation, extensions and conclusion.

To analyze the drag configuration of the dimpled golf ball using changing wind velocities and other features such as pressure and velocity configuration on the ball and the dimples, the process of how air flow passes through a dimpled ball's surface will be introduced. During the ball flight, two types of drag are in effect, i.e., pressure drag and viscous drag [9]. The pressure difference in the front and back of the ball causes pressure drag. The viscous drag is due to the shear stress along the boundary of the ball. In the golf ball scenario, pressure drag is more significant, as there is a significant pressure difference in the front and back of the ball. The pressure difference is caused by flow separation.

When the air encounters the ball, there is an air stagnation point in the front, where the pressure is the greatest. Air sticks to the ball because of the no-slip condition caused by viscous forces. Outside the boundary layer is the undisturbed free stream. Because of viscosity, the airstream in the boundary layer flows slower than the freestream. However, because of the high pressure at the air stagnation point, there is a favorable pressure gradient relative to the distance on the ball surface that increases the velocity gradient of the airstream in the boundary layer. When the airstream moves across the top, there is a reverse pressure gradient, hindering the airstream movement around the ball. When the velocity of the airstream near the surface is decreased to zero and below, the flows separate and deviate from the surface, generating a wake region that drops the pressure [9]. Because the front of the ball has higher pressure while the back has lower, a resistance force is exerted on the ball in the backward direction, which is the aerodynamic pressure drag. This process varies in the case of smooth balls and dimpled balls.

On the smooth ball, there is a laminar boundary layer on the ball's surface, where air moves smoothly together because the ball's surface is flat and there are no disturbances. Air moves steadily and relatively slowly so that there is no exchange of kinetic energy with the free stream above it. After passing the separation point, the boundary layer airstream has difficulty attaching to the ball's surface because the reversed pressure gradient decreases its velocity, causing the flow to separate early. This creates a large wake region behind the ball, which causes the drag force on the smooth ball to be significant. For a dimpled ball, rather than having a laminar boundary layer on its surface, it has a turbulent boundary layer. The layer is formed due to the small vortices generated on top of the dimples that disturb the steady laminar boundary layer [4]. In this case, the air in the boundary layer interacts with the free stream on top of it to retain more kinetic energy due to its instability. The greater kinetic energy allows the airstream to resist the reversed pressure gradient, maintaining its velocity longer and thus delaying the flow separation. This causes the wake region behind the ball to decrease since the air flows are less separated. This way, pressure in the wake is maintained, lowering the pressure difference between the ball's front and back, thus decreasing the pressure drag.

The drag equation deriving from Bernoulli's equation is commonly known to relate the velocity of the object to the drag force it experiences [7].

$$F_{drag} = \frac{1}{2}\rho v^2 C_D A \tag{1}$$

Where $\rho$ represents the density of fluids, v is the velocity of the object, $C_D$ is the drag coefficient and A is the cross sectional area of the object. The equation applies to the body moving through fluids under a high Reynolds number, meaning that the system is turbulent and is descriptive of the golf ball case. The formula suggests a quadratic relationship between the drag force and velocity, suggesting that as wind velocity increases, the drag force experienced by the golf ball increases quadratically.

However, as discussed in the previous paragraph, the role of dimples is to disrupt the laminar boundary layer attached to the ball's surface to induce kinetic energy exchange with the free stream. Due to the difficulty of studying the three-dimensional flow around dimples, quantitative analysis of how much a dimple disrupts the flow would be unlikely to be conducted. However, it is reasonable to hypothesize that the faster the airflow travels, the more quickly they can be separated, thus inducing a greater wake region and, thus, a more significant drag force. However, with the dimples, the airstream that obtains greater momentum from the higher pressure at the air stagnation point becomes more easily disrupted. This is reasonable since a fast-moving airstream is more turbulent than a slow-moving one, so the dimples can have a greater effect on resisting the reverse pressure gradient. In this case, kinetic energy exchange is more efficient, reducing the increase of the wake region.

Due to the above reasons, it is hypothesized that the dimpled golf ball follows the drag formula generally, meaning that as wind velocity increases, the drag increases approximately quadratically. However, because of the dimples' effect, the drag force's rate of change decreases, meaning that the drag force will not be to the second power of velocity but slightly lower. Apart from this, since the main drag is contributed by pressure, it is hypothesized that the pressure difference across the ball also increases approximately quadratically with changing wind velocities. It is also expected to see the exchange of kinetic energy on the golf ball's surface and the vortices on the dimples and in the wake region behind the ball in the flow simulation.

## 2. Methodology

In this experiment, Ansys fluent is used to model the drag that the golf ball experiences and the pressure and distribution on the golf ball in varying wind velocities. This software was chosen due to its capacity to model turbulence and fluid structure modeling. It is downloaded directly from the official website and installed following the instructions available. In order to simulate the drag force experienced by the golf ball in wind, the ball should be placed inside a certain geometry as the flow field. Inside the flow field, CFD can be conducted to monitor the parameters related to the ball, other environmental factors(such as temperature, viscosity of air) and the independent variable in this experiment, i.e., wind velocity. To begin with, a 3-D dimpled golf ball geometry was downloaded from the CFD website [10] and opened in Spaceclaim. In this, the golf ball structure was embedded in a 3-D rectangular flow field in which the aerodynamics of the golf ball was visualized (seen from Fig. 1).

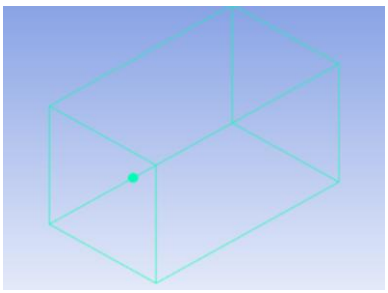

**Figure 1.** The visual representation of the dimpled golf ball and space around it in Ansys fluent software

Next, a mesh is constructed. Meshing is a process that divides a continuous body into a finite amount of blocks. Due to the complexity of the continuous 3-D structure of the golf ball, computers cannot perform calculations on an undetermined surface. However, it can solve partial differential equations on predictable shapes and mathematically defined volumes. Meshing is essential since this

study is closely simulating the flows on the golf ball surface. Thus, the combined structure was induced into meshing. The mesh quality was adjusted appropriately so that the simulation would be accurate and time-saving. The Fig. 2 and Fig. 3 are the specific parameters and settings for the mesh of the surface, flow field and inflation, which is the high-quality mesh on the surface of investigation.

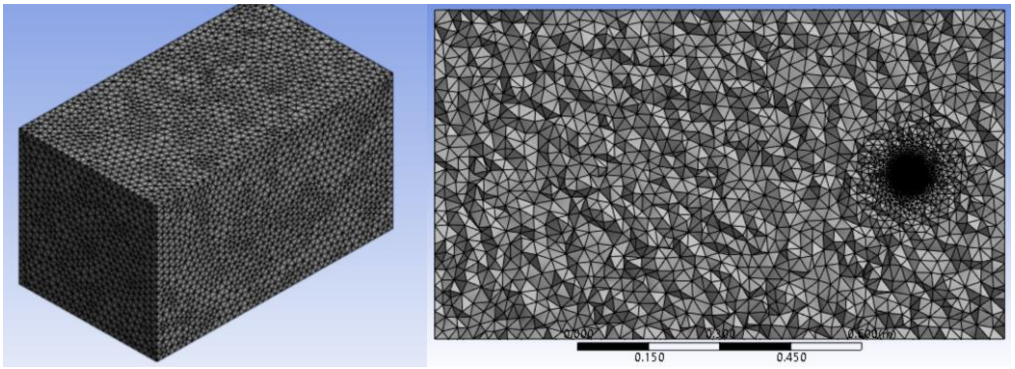


**Figure 2.** An 3-D view of the outside and the cross-section of the flow field mesh

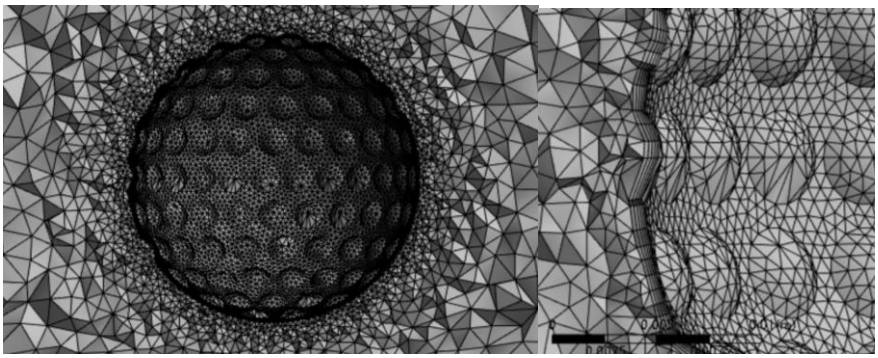

**Figure 3.** The magnified view of the golf ball mesh and the inflation layers

With the generated mesh, one can calculate the drag force and model the flow in fluent software. In reality, wind and the golf ball are separate objects, each possessing velocities. However, for convenience in the experiment, the ball's velocity will be set as zero, and the wind velocity is varied accordingly since velocity is relative. In Meshing, one named surfaces of the geometry. As shown in Fig. 4, the blue rectangular surface is the inlet, where the wind enters, and the red outlet surface is where the wind exits. The simulation takes place between the surfaces.

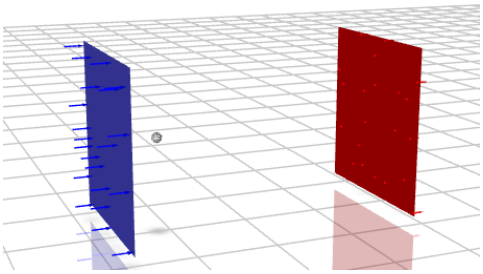

**Figure 4.** The visual representation of the inlet surface, outlet surface and golf ball in the flow field geometry

Subsequently, other experiment-related settings were finalized as suggested by the CFD instruction video [11]. Since the golf ball travels in air, the material type is selected as air. The density and viscosity of air was set constant and the specific values were 1.225 $kgm^{-3}$ and $1.802 \times 10^{-5} kgm^{-1}s^{-1}$, based on air characteristics at 15 degree celsius for generalization [12]. Next, in the "inlet" of in the Boundary Conditions section, the velocity magnitude is adjusted based on the nine wind velocity values selected in this experiment: 40, 30, 20 10, 0, -10, -20, -30 and -40 $ms^{-1}$. It is worth mentioning that relative velocity is used, with the golf ball velocity chosen as $75ms^{-1}$ [13]. Thus, the nine inlet relative velocity values are 115, 105, 95, 85, 75, 65, 55, 45 and 35

$ms^{-1}$ since the ball is held still. In the initiation, the Z velocity is adjusted based on the inlet velocity. After initializing the program, this study performed a calculation with 200 iterations for each data point since Ansys CFD uses an iterative approach to reach simulation results. When the calculation was complete, following information was noted: the figure of static pressure of air, the figure of air stream velocity magnitude, the vector figure of air stream velocity magnitude indicating the direction of airflow, and the specific values of pressure drag, viscous drag and total drag. For experimental controls of unrelated variables, only the velocity magnitude in "inlet surface" setting and value of "Z velocity" in initialization are changed when a new wind velocity is tested, while all other parameters stay constant.

## 3. Results and Discussion

### 3.1. Drag Comparison

As demonstrated in the Table. 1 and Fig. 5, as the wind velocity increases, pressure drag, viscous drag and net drag all show a steady increase. For pressure drag, the modeling is chosen as $AW^B$. Tis equation can test if the hypothesis is valid by showing the general trend and the rate of change. In this computer generated model, the equation is represented as $0.0001639W^{2.042}$. The 2.042 index suggests a positive quadratic relationship between wind velocity and pressure drag. So, as wind velocity increases, the drag experienced by the ball increases quadratically. The correlation is 0.9967, meaning the model is highly appropriate for the collected data. The modeling results partly comply with the hypothesis that drag increases approximately quadratically with higher wind velocity. However, the rate of change increases, as demonstrated by the model index, rather than decreasing as predicted previously. A possible explanation is that as the golf ball runs into the wind faster, the wake region behind the ball increases significantly. While the hypothesis of the more turbulent airstream reducing the wake region could be true, and this could be determined by looking into the simulated airstream configuration in the next section, it is reasonable to conclude that the faster wind velocity increases the wake region more significantly, resulting in a positive rate of change.

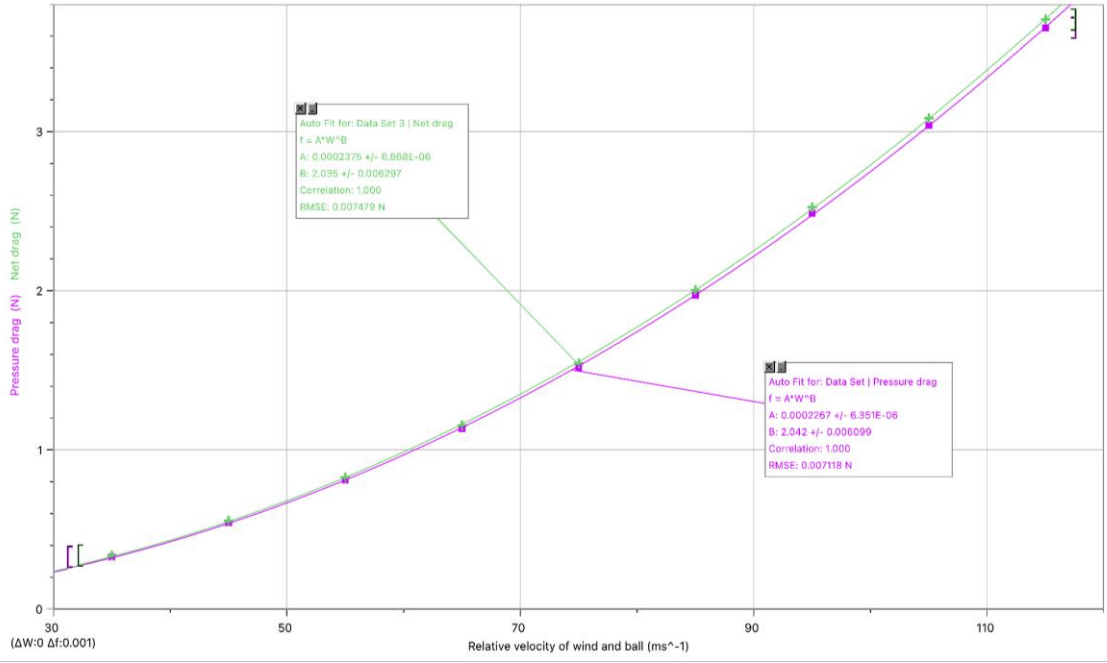


**Figure 5.** The pressure drag [N] with varying relative velocity of the wind and the ball [$ms^{-1}$]. A computer generated power fit(violet) in the form of $AW^B$. The net drag [N] with varying relative velocity of the wind and the ball [$ms^{-1}$]. A computer generated power fit(green) in the form of $AW^B$

Similar trend is observed for the figure of net drag, in which the the modeling equation is $0.0002375W^{2.035}$. As shown in the index, 2.035, the net drag also increases quadratically with increasing wind velocity. At the same time, the relationship is even closer to an entirely quadratic one, which is more consistent with the drag equation. It is also determined that although it is said that the dimples reduce drag, they still comply with the drag equation and do not affect the pattern described in it. The correlation is 1.000, suggesting that the equation models the data accurately. The viscous drag is an insignificant component of the experiment due to its small magnitude.

**Table 1.** The ball velocity $ms^{-1}$, wind velocity $ms^{-1}$, relative velocity $ms^{-1}$, air density $kgm^{-3}$, viscosity $kgm^{-1}s^{-1}$, pressure drag [N], viscous drag [N] and net drag [N] of the golf ball, with the relative velocity ranging from $115ms^{-1}$ to $35ms^{-1}$ with $10ms^{-1}$ interval

| Wind velocity $ms^{-1}$ | Relative velocity $ms^{-1}$ | Pressure drag [N] | Viscous drag [N] | Net drag [N] |
|---|---|---|---|---|
| 40 | 115 | 3.652 | 0.052 | 3.705 |
| 30 | 105 | 3.040 | 0.045 | 3.084 |
| 20 | 95 | 2.487 | 0.038 | 2.525 |
| 10 | 85 | 1.973 | 0.031 | 2.004 |
| 0 | 75 | 1.518 | 0.026 | 1.543 |
| -10 | 65 | 1.134 | 0.020 | 1.154 |
| -20 | 55 | 0.812 | 0.016 | 0.828 |
| -30 | 45 | 0.543 | 0.012 | 0.555 |
| -40 | 35 | 0.033 | 0.009 | 0.337 |

### 3.2. Static Pressure Configuration

After quantifying the drag force experienced by the golf ball with $75ms^{-1}$ velocity into wind with -40 to $40ms^{-1}$ velocity, one can take a closer look into the static pressure distribution around the golf ball. The fluent simulation displays the static pressure configuration in Fig. 6 that indicates its magnitude. The diagram of the golf ball with $75ms^{-1}$ relative velocity will be discussed as an example. As shown, the pressure is the highest at the air stagnation point, the front of the golf ball, where the region is coloured bright red. The pressure gradually decreases to negative at approximately the top, indicating a reverse pressure gradient as described in the theoretical analysis, where the pressure is the minimum. The region behind the ball also clearly shows a low-pressure zone. There is an obvious indication of pressure difference before and after the ball, contributing to the pressure drag. The simulation results fit the hypothesis about pressure distribution on the golf ball that the pressure is the greatest airflow that first encounters the front of the ball and decreases to create the wake region behind the ball. Before analyzing the effect of wind velocity on the pressure configuration numerically, it is worth noting that all the pressure measurements displayed by the fluent software are the gauge pressure. In this experiment, the operating pressure is set as the atmospheric pressure, so the negative pressure value does not necessarily mean the pressure is below zero at that region.

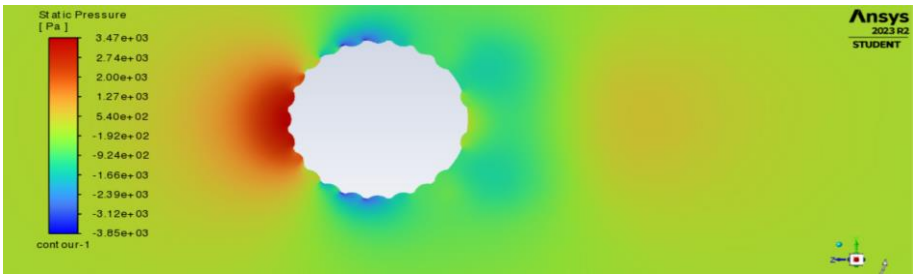


**Figure 6.** A visualization of the pressure distribution on a golf ball with coloured indication of magnitude of pressure

The pressure configuration of all other wind velocities is very similar to that of the $75ms^{-1}$ one. The magnitude of pressure varies when the wind velocity changes, and they are quantified by fluent, as shown in table 2. However, the pressure presented is continuous, as the color represents a range of pressure values. For convenience, the pressure at the front of the ball will be calculated by averaging the three values of the three most apparent colors on the color bar. As shown in Table 2 and Fig. 7, when wind velocity increases, the front pressure, the magnitude of the back pressure and the pressure difference increase. The upward curve demonstrates this fit with the modeling equation as $AW^B$. The 2.009, 1.968 and 2.001 index of front, back and difference of pressure suggest a quadratic relationship, which helps explain the quadratic pattern observed in drag force since the pressure difference is the significant contribution.

**Table 2.** The wind velocity from 35 to $115ms^{-1}$, front pressure, back pressure, back pressure magnitude and pressure difference all in pascal in the displayed pressure configuration diagrams

| Wind velocity $[ms^{-1}]$ | Front pressure [pa] | Back pressure [pa] | Back pressure magnitude [pa] | Pressure difference [pa] |
|---|---|---|---|---|
| 35 | 592 | -156 | 156 | 748 |
| 45 | 978 | -257 | 257 | 1234 |
| 55 | 1463 | -387 | 387 | 1850 |
| 65 | 2050 | -525 | 525 | 2575 |
| 75 | 2737 | -681 | 681 | 3417 |
| 85 | 3530 | -811 | 811 | 4341 |
| 95 | 4407 | -1029 | 1029 | 5435 |
| 105 | 5380 | -1300 | 1300 | 6680 |
| 115 | 6457 | -1583 | 1583 | 8040 |

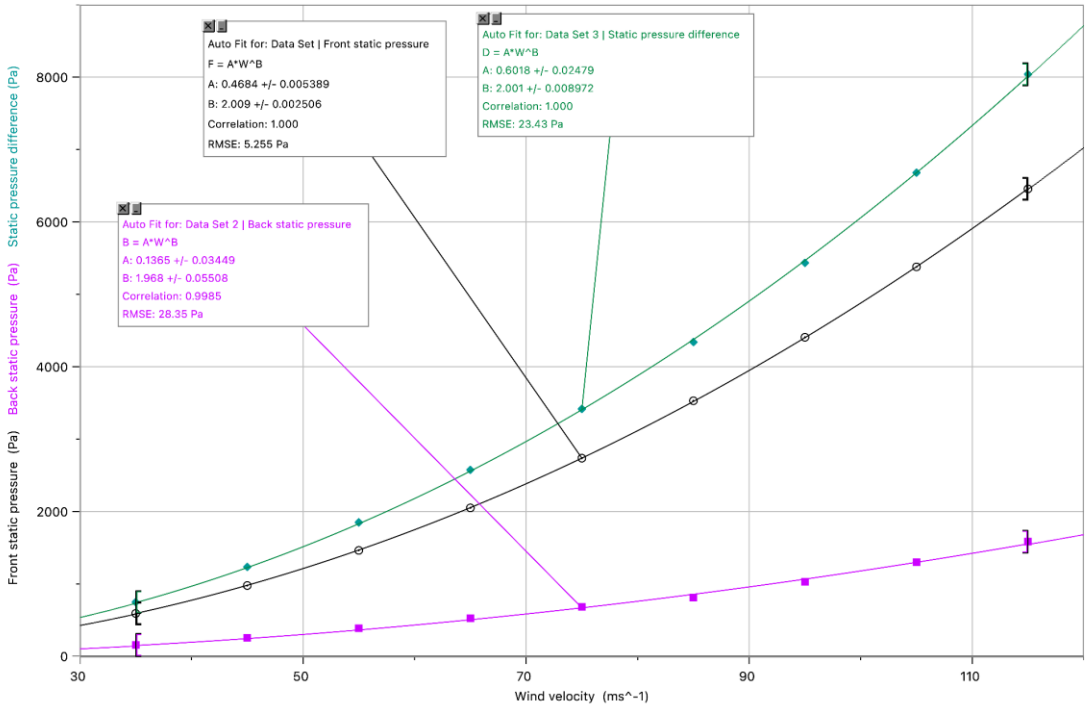


**Figure 7.** The data points and curve fits of front pressure, magnitude of back pressure and pressure difference on the golf ball, with correlation indicated

### 3.3. Air Stream Velocity Configuration

The air stream velocity configuration describes the magnitude and direction of the airflow on the golf ball surface as well as in the surrounding space. The simulation generated at the relative velocity of $75ms^{-1}$ will be presented as an example, and the configurations at other data points are similar to the exemplar which will be presented in the appendix section. The velocity configuration will be analyzed generally, describing its macroscopic distribution, and specifically by looking into the details on the dimples to see how they disturb the airflow to transfer the laminar flow into the turbulent one.

Fig. 8 shows that the velocity is the lowest at the air stagnation point and behind the ball. At the air stagnation point, the pressure is the highest, and because of the high static pressure, the air cannot move freely, accounting for the low velocity. The positive pressure gradient gradually increases the air stream velocity across the surface, as the red color suggests. After moving through the top of the ball, the fast-moving airstream has difficulty attaching to the ball's surface, as layers of distinct colors of red, blue and green can be observed. The fast-moving airflow, identified by its reddish color, remains separated from the region behind the ball, clearly identifying a low velocity and pressure zone—the wake. The flow intensity in this region is low and insignificant, and there are recirculating flows and vortices indicated by the reversed velocity vector and circular flow pattern. The macroscopic features of the velocity configuration fit the descriptions in the theoretical analysis.

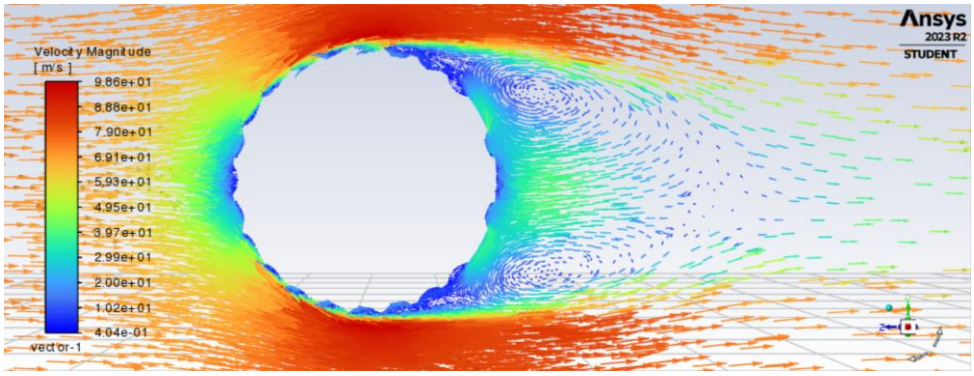


**Figure 8.** The simulation of velocity (both magnitude and direction) of the golf ball at the relative velocity of $75ms^{-1}$

It is acknowledged that the vortices above each dimple transform the laminar flow into turbulence by disturbing its stability and inducing kinetic energy exchange with the fast-moving airstream outside. In this simulation, the effect of the dimples can also be visually presented. This exemplar is chosen from the dimple on the top of the ball with a relative velocity of $75ms^{-1}$. As shown in Fig. 9, the fast-moving airflows, represented by the red arrows, are on the outside. In dimples, vortices and low-velocity airflow travel in the opposite direction of the red arrows and are in a circular configuration. These could be the vortices generated by the dimples. Based on the vector configuration, the vortices disturb the initially more stable airflow, as the color of the airstream velocity on the left side is generally low, represented by the green color. As the vortices disturb the laminar flow, components shift from green to red, suggesting that the airstream gains kinetic energy, becoming more turbulent. When wind velocity increases, the velocities of both the fast-moving and circular flows on the dimples increase, resulting in a more significant exchange of kinetic energy. It corresponds to the predictions of the dimple's effect in the theoretical analysis section.

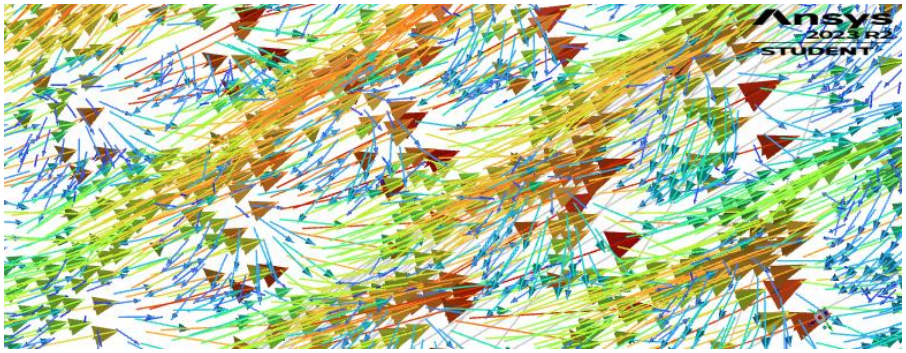


**Figure 9.** The view of airstream velocity vectors on the dimples from the inside of the golf ball

## 4. Evaluations

Although the experimental results are promising, there are a few limitations to this research. Firstly, the scope of the investigation is limited. In a realistic situation, the golf ball will not fly entirely in the horizontal direction. The situation simulated in this experiment requires the golf ball to travel ideally horizontally in the direction of the wind, which is rare in reality. The flow configuration and pattern observed in drag force thus reflected only the result in the strictly controlled conditions. The characteristics of air are also inconsistent with realistic conditions. During the golf ball's flight, the air it travels in is not equally viscous and dense, and its specific values are affected by elevation and geographic location. In this experiment, the air is also regulated at 15 degrees Celsius, which varies considerably. Thus, the pattern discovered in this experiment can vary or might be less applicable to reality because the experimental parameters are indefinite.

Additionally, this simulation cannot conduct a quantitative analysis of the effect of dimples as part of the aim of the research to analyze the aerodynamic details. This is difficult because each dimple has a different orientation, and air can flow irregularly. It is also too time-consuming to separate each dimple and perform CFD on each since a golf ball typically has over 300 dimples. Besides, since a golf ball geometry file is directly downloaded from a professional CFD website, its geometric specifications are unknown, i.e., the number of dimples, the length and depth of dimples, the material and the mass of the ball. While it is ideal to be aware of this information when performing quantitative analysis, it upholds the quality of exploration in this specific experiment. However, with information such as the ball's mass, the ball's acceleration at each instant can be modeled, and if the initial launch angle and spin are set, the golf ball's trajectory can be graphed.

To further understand the aerodynamic process of the golf ball, an experiment that compares the specifics of a smooth ball and a dimpled ball should be conducted to analyze the effect of dimples. If both smooth ball and dimple ball conform to the drag equation, it is intriguing to investigate how they differ. To further study the effect of dimples quantitatively as a unique aerodynamic structure, an experiment can also be conducted to investigate the effect of changing dimple quantities on a golf ball. This furthers the qualitative examination of the dimple's effects in this experiment.

## 5. Conclusion

In conclusion, it is found that the drag force of a dimpled golf ball conforms to the pattern in the drag equation. As wind velocity increases, the net drag forces experienced by the golf ball increase approximately quadratically with an index of 2.035. The net drag mainly consists of pressure increases with an index of 2.042. All results suggest that the drag equation can be used to model the drag force experienced by a dimpled golf ball during its flight, regardless of the effect of the dimples. A significant pressure difference at the front and back of the ball is observed, which also increases quadratically with greater wind velocities. The distribution of pressure also aligns with the theoretical analysis. The velocity distribution of airflows passing through the ball’s surface corresponds to the pressure distribution. Finally, regarding the flow pattern on top of the dimple, it is consistent that the

laminar flow is disturbed by the vortices generated on the dimple and transformed into turbulent flow with greater velocity. This research models the air flow and drags on a sphere with dimpled geometry, and it sheds light on whether such geometry will affect the aerodynamic behavior, such as the drag of other objects. The findings describe the airflow on a dimpled geometry in great detail and can inspire the application of such geometry in other fields.

## References

[1] Jenkins P E, Arellano J, Ross M, Snell M. Drag coefficients of golf balls. World Journal of Mechanics, 2018, 08(06): 236–241.

[2] Veilleux T. How do dimples in golf balls affect their flight. Scientific American, 2005, Retrieved from: https://www.scientificamerican.com/article/how-do-dimples-in-golf-ba/.

[3] Cunningham K. How many dimples on a golf ball. Golf, 2019, Retrieved from: https://golf.com/gear/golf-balls/how-many-dimples-on-a-golf-ball/.

[4] Choi J, Jeon W P, Choi H. Mechanism of drag reduction by dimples on a sphere. Physics of Fluids, 2006, 18: 4.

[5] Alam F, Steiner T, Chowdhury H. et al. A study of golf ball aerodynamic drag. Procedia Engineering, 2011, 13: 226–231.

[6] Chowdhury H, Loganathan B, Wang Y. A study of Dimple characteristics on golf ball drag. Procedia Engineering, 2016, 147: 87–91.

[7] Seeley J M, Crosser M S. The Drag Coefficient of Varying Dimple Patterns. Digital Commons, 2018.

[8] Tai C H, Leong J C, Lin C Y. Effects of golf ball dimple configuration on aerodynamics, trajectory, and Acoustics. Journal of Flow Visualization and Image Processing, 2007, 14(2): 183–200.

[9] Artola B. Why do golf balls have dimples. COMSOL, 2021. Retrieved from: https://www.comsol.com/blogs/why-do-golf-balls-have-dimples/.

[10] Main Resource of Computational Fluid Dynamics. (n.d.). Dimple Bal Geometry File. Falmouth, 2010.

[11] MR-CFD ANSYS Fluent Training. ANSYS FLUENT TRAINING: Golf ball Aerodynamics, CFD Simulation by ANSYS Fluent, 2021. Retrieved from: https://www.youtube.com/watch?v=ZZk32wQ7-GE.

[12] Edge E. Viscosity of air, dynamic and Kinematic. Engineers Edge - Engineering, Design and Manufacturing Solutions. Engineers Edge LLC: Monroe, GA, USA, 2020.

[13] Foresight Sports. (2019, August 21). What is Ball Speed in golf: Breaking down the Data. Foresight Sports, 2019, Retrieved from: https://www.foresightsports.com/blogs/golf-tips/what-ball-speed-golf-breaking-down-data.